

# Novel methods for preparing phospholipid coated microbubbles

K. P. Pancholi · U. Farook · R. Moaleji ·  
E. Stride · M. J. Edirisinghe

Received: 23 April 2007 / Revised: 6 July 2007 / Accepted: 10 July 2007 / Published online: 9 August 2007  
© EBSA 2007

**Abstract** Two new methods for preparing phospholipid coated microbubble suspensions are elucidated. Firstly, co-axial electrohydrodynamic atomisation was utilized to generate 3–7  $\mu\text{m}$  diameter microbubbles. Secondly, a specially designed and constructed T-junction device was used to prepare monodisperse microbubbles. Characteristics of microbubbles prepared by these two methods are compared with those obtained by sonication of the phospholipid suspension.

**Keywords** Phospholipid · Microbubbles · Electrohydrodynamic · T-junction

## Introduction

Phospholipid-coated microbubbles are employed in a number of important medical applications: they have been shown to be very effective as contrast agents for diagnostic ultrasound imaging and, more recently, as vehicles for targeted drug and gene delivery (Talu et al. 2006; Unger et al. 2004; Stride and Saffari 2003; Dayton and Ferrara 2002). One of the most important factors determining the response of a coated microbubble to ultrasound excitation is its size. For drug-delivery applications in particular, a well-defined microbubble size distribution is a critical requirement in order to ensure correct dosage. A prerequisite for using microbubbles for either contrast enhancement or drug

delivery is that they are biodegradable and the largest bubble diameter does not exceed 10  $\mu\text{m}$ , in order to avoid the risk of embolism (Unger et al. 2001). The required level of control in size and size-distribution is not provided by existing microbubble preparation techniques. Thus, over-size bubbles have to be removed by costly and cumbersome post-preparation treatments.

Existing methods for the manufacture of coated microbubble suspensions involve the production of gas bubbles in a solution containing a suitable surfactant such as a mixture of phospholipids or serum albumin. The surfactant forms a coating on the surface of the bubble, which counteracts surface tension thus stabilising the bubble and preventing rapid dissolution. In order to prepare microbubble suspensions, gas is usually entrained by agitation, sonication or high shear mixing, in a liquid containing the material that is to coat the surface of the bubble. This most commonly used method has the disadvantage of producing a broad size distribution of microbubbles, a significant proportion of which are  $>10 \mu\text{m}$  in diameter, and must therefore be filtered or fractionated (Klibanov 1999). Microbubbling can also be carried out with microfluidic flow focusing devices produced using sophisticated soft-lithography techniques (Hettiarachchi et al. 2007). Other methods used to prepare microbubble suspensions include spray drying and solvent evaporation but these are considered to be too complicated owing to the large number of processing steps involved (Unger et al. 2001).

Recently, we used co-axial electrohydrodynamic atomization for the first time to prepare microbubble suspensions with a model glycerol-air system and reported that suspensions of microbubbles smaller than 10  $\mu\text{m}$  in diameter with a narrow size distribution can be generated by achieving the microbubbling mode (Farook et al. 2007a, b). In this letter, we elucidate how co-axial electrohydrodynamic microbubbling

---

K. P. Pancholi · U. Farook · R. Moaleji · E. Stride ·  
M. J. Edirisinghe (✉)  
Department of Mechanical Engineering,  
University College London, Torrington Place,  
London WC1E 7JE, UK  
e-mail: m.edirisinghe@ucl.ac.uk

is used to prepare 3–7  $\mu\text{m}$  diameter phospholipid coated microbubble suspensions. Also, we demonstrate how a specially designed and constructed T-junction device was used to prepare perfectly monodisperse microbubbles.

### Experimental details

The constituents and the amounts used in this study were deduced from the work of Talu et al. (2006) who investigated an optimised composition for microbubble production by flow focussing. 0.25 g of the phospholipid hydrogenated L- $\alpha$ -phosphatidylcholine (white crystalline powder,  $\geq 99\%$  purity,  $\text{C}_{40}\text{H}_{80}\text{NO}_8\text{P}$ , relative molecular mass 734), 0.071 g of polyethyleneglycol 40 stearate-40 (density  $1,300 \text{ kg m}^{-3}$ ), 25 ml of glycerol (density  $1,260 \text{ kg m}^{-3}$ ) and 25 ml of propane-1,3-diol (density  $1,000 \text{ kg m}^{-3}$ ), was mixed with 50 ml of distilled water in a conical flask using slow magnetic stirring (all constituents were purchased from Sigma-Aldrich Co. Ltd. Dorset, UK). Subsequently, the flask was topped up with distilled water to the 250 ml mark. The mixture was then stirred for 300 s but this resulted in a suspension containing undispersed lipid.

To achieve lipid dispersion, the suspension was sonicated using a Misonix ultrasonic cell disruptor XL200 (Labcaire Systems Ltd. Somerset, UK) working at 12 W for 60 s. Care was taken to avoid creating bubbles while sonicating by placing the ultrasonic probe deep in the solution (the lack of bubbles was confirmed by ultrasound characterisation as described below). A smaller volume of the suspension was taken in a test tube and was sonicated again at the same power output for a further 120 s with the probe deep in the sample before removing 5 ml of the sample at a time in a syringe for electrohydrodynamic and T-junction bubbling experiments (see below). A sample was also taken from the 250 ml aliquot and sonicated in a beaker at 7 W (level 4) for 30 s with the ultrasonic probe at the top of the container, to prepare microbubbles, which were taken on glass microscope slides and immediately studied by optical microscopy.

The density of the lipid suspension was measured using a standard density bottle technique, viscosity was estimated using a VISCOEASY rotational viscometer, electrical conductivity was assessed using a standard conductivity probe and surface tension was measured using the Kruss Tensiometer (plate method). All experiments were performed at room temperature after calibrating the equipment using distilled water.

The experimental rig used for co-axial electrohydrodynamic atomization (Fig. 1) consisted of a pair of stainless steel needles arranged concentrically. The inner needle had 150  $\mu\text{m}$  inner diameter (ID) and 300- $\mu\text{m}$  outer diameter (OD). The outer needle dimensions were 685  $\mu\text{m}$  ID and

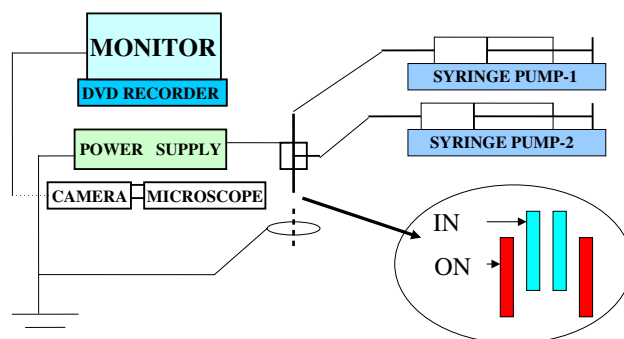


**Fig. 1** Schematic representation of the equipment set-up for the generation of microbubbles by co-axial electrohydrodynamic atomization. *IN* and *ON* indicate inner and outer needles, respectively

1,100  $\mu\text{m}$  OD. Both needles were connected to the same applied voltage source and an earthed ring electrode (ID 15 mm and OD 20 mm) placed 12 mm below the tip of the outer needle. The inner needle exit was placed  $\sim 2$  mm above the tip of the outer needle. This facilitates encapsulation of the air by liquid (Farook et al. 2007a, b). Air was pumped through the inner needle and the phospholipid suspension through the outer. The air and liquid flow rates were controlled by high precision Harvard syringe pumps using plastic syringes, 10 and 5 ml volume capacity, respectively. The flow exiting the needles was monitored on a screen using a LEICA S6D JVC-colour video camera attached to a zoom lens and a data DVD video recorder MP-600 using CDV Recorder/Editor DN-100. The microbubbles produced were collected just below the ring electrode on glass microscope slides and immediately studied by optical microscopy.

The details of the specially designed and constructed T-junction (Fig. 2) are as follows: the ends of two capillaries having 150  $\mu\text{m}$  internal diameter were axially aligned and encased within a rigid polymer block (10 mm thick) separated by a distance of 70  $\mu\text{m}$ . A third tube was inserted into the polymer block so that it was perpendicular to the axis of the other two tubes to facilitate a complete T-junction. Each tube was secured mechanically to the block in a fashion that

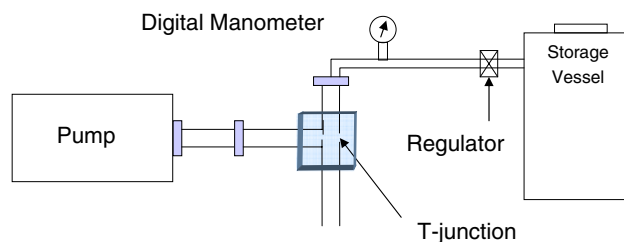


**Fig. 2** Schematic representation of the equipment set-up for the generation of microbubbles by the specially designed T-junction

it could take maximum pressure without slipping away from the junction. This design was found to be both robust and rigid, withstanding the very high pressures generated at the T-junction (up to 600 kPa). The top tube of the T-junction was connected to a pressurised vessel supplying gas at constant pressure (measured by a digital manometer connected to the top tube) whereas the tube perpendicular to the top tube was connected securely using leak proof mechanical coupler to a 20 ml stainless steel syringe (KD Scientific, Holliston, MA, USA). The phospholipid suspension was supplied to the T-junction using a Harvard syringe pump to maintain a constant flow rate.

In these experiments liquid flow rate was maintained at  $8.3 \times 10^{-9} \text{ m}^3/\text{s}$  and air pressure was maintained at 25 kPa. Basically, the air pressure was increased to counter liquid from flowing upstream of the junction. As air pressure is increased, the air stream starts breaking up at constant rate and this event is repeatable. If air pressure continues to be increased, ultimately atomization of liquid is observed, whereas below this threshold bubbling is present. It is important to increase air pressure very gradually to ensure that the air jet was surrounded by liquid at the T-junction. Sudden increase in air pressure can even shut down the liquid supply to the junction. Taking liquid viscosity ( $\sim 3 \text{ mPa s}$ ) into account, liquid flow rate was kept at  $8.3 \times 10^{-9} \text{ m}^3/\text{s}$ . For high viscosity liquids ( $> 50 \text{ mPa s}$ ) 1/10 of this flow rate is recommended as the liquid pressure required to bubble decreases with increasing liquid viscosity. Air pressure was also subjected to further fine control in the 0.1–1.5 kPa range to counteract dynamic pressure change in the syringe pump. The microbubbles prepared by this method were collected at the end of the third (outlet) tube of the T-junction in a vial containing distilled water. Subsequently, microbubble samples were taken on to glass slides and investigated via optical microscopy.

In addition to optical microscopy, ultrasonic characterisation was also carried out on samples of microbubbles prepared by each of the different techniques. This was done for two reasons. Firstly, it was important to confirm that microbubbles (as opposed to liquid-filled liposomes) had definitely been formed and the difference in ultrasound scattering between gas bubbles and solid or liquid particles<sup>1</sup> is far greater than the difference in their optical appearance. Secondly, it was desirable to see whether it was possible to determine any differences in the acoustic response of microbubbles prepared using the three different techniques.

For each measurement, 1 ml of the prepared microbubble suspensions was added to a specially designed chamber filled with distilled water. The chamber was constructed from a section of PMMA (polymethylmethacrylate) tubing

(inner diameter 60 mm, wall thickness 5 mm, length 30 mm) with acoustic “windows,” made from polyethylene film (thickness 50  $\mu\text{m}$ ), at either end. The tubing was held between two square aluminium plates into which recessed circular holes had been cut to allow access to the ends of the tubing and hold it in place. The chamber was suspended in a water bath, also filled with distilled water, to enable transmission of the ultrasound through the chamber and to minimise fluctuations from the ambient temperature.

Measurements of ultrasound propagation through the microbubbles in the chamber were made using a custom made broadband transducer having a nominal centre frequency of 5 MHz, diameter 20 mm and a 3 dB bandwidth of 5 MHz. This was positioned above the upper window of the chamber so that the ultrasound beam passed through the chamber on to a stainless steel reflector on the base of the tank and back to the transducer. The distance between the transducer face and the steel plate was 60 mm. The transducer was activated using a pulser/receiver unit (Panametrics model 5055 PR), which was set to give an output peak negative pressure in water of approximately 50 kPa. The exact pressure was determined using a needle hydrophone. Signal capture was performed using a digital oscilloscope (LeCroy 9310M Dual 300 MHz) which was connected via GPIB to a PC running data analysis software written in MATLAB version 7 of 2006 release A implementing a 2D Hough transformation algorithm.

## Results and discussion

The measured properties of the phospholipid suspension are given in Table 1. The suspension was found to be approximately three times as viscous as water, surface tension was  $\sim 60\%$  that of water and the electrical conductivity was  $\sim 90\%$  that of distilled water. These properties are crucial to the electrohydrodynamic behaviour since the reduction in surface tension will help the electrical forces to generate a jet, whilst the increase in viscosity will have the opposite effect (Jayasinghe and Edirisinghe 2002).

The reduction in equilibrium (static) surface tension is beneficial in the generation of the microbubbles. However, estimation of the dynamic surface tension would have allowed a greater understanding of microbubble dynamics (Hallowell and Hirt 1994). Dynamic surface tension is

**Table 1** Properties of the lipid suspension prepared for microbubbling experiments, error in measurements are expressed as a %

Density	1,030 $\text{kg m}^{-3}$
Viscosity	$2.6 \pm 1.9 \text{ mPa s}$
Surface tension	$43 \pm 0.46 \text{ mN/m}$
Electrical conductivity	$8.8 \pm 11.4 \mu\text{S/m}$

<sup>1</sup> The scattering cross-section of a gas bubble may be several orders of magnitude greater than a liquid sphere of the same size.

important in tracking changes continuously during surface formation, an important consideration when surfactants are present. Dynamic measurements can track when the highest surface tension occurs, at which point none of the surfactant molecules have aligned at a surface, to equilibrium conditions coinciding with the lowest surface tension when no additional surfactant molecules can be added to the surface.

Figure 3 shows an optical micrograph of the microbubbles prepared by sonication and clearly shows the presence of a very wide size-distribution of microbubbles ranging from a few micrometers in size to  $\sim 50 \mu\text{m}$ .

Co-axial electrohydrodynamic microbubbling was carried out at various flow rates and applied voltages (Table 2). When no electric field was applied, very coarse microbubbles  $>500 \mu\text{m}$  were obtained. The application of an electrical field causes bubble dripping to transform to the coning mode and eventually to the microbubbling mode, with increasing applied voltage (Fig. 4). Microbubbles with size  $<10 \mu\text{m}$  were obtained at air and lipid flow rates of 1,200 and  $300 \mu\text{l min}^{-1}$ , respectively, in the voltage range 7.2–8.5 kV (Table 2). However, the size of microbubbles at 9.5 kV for all combinations of flow rate show that the bubble size begins to increase beyond a certain range of applied

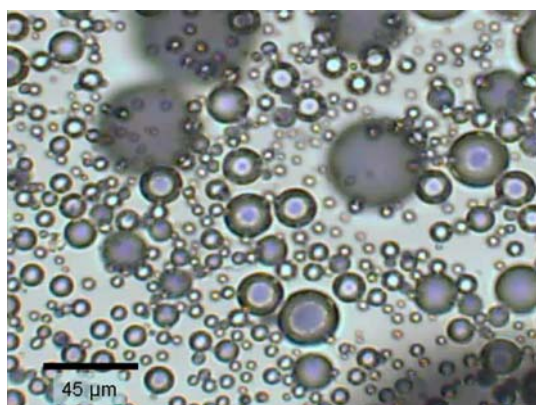


**Fig. 3** Optical micrograph of the bubbles generated by sonication

**Table 2** Microbubble sizes obtained by co-axial electrohydrodynamic flow, error in measurements are expressed as a %

Applied voltage/ kV	Bubble size/ $\mu\text{m}$			
	Flow rate/ $\mu\text{l min}^{-1}$ , air–lipid suspension			
	300–300	600–300	900–300	1,200–300
0	$580 \pm 2.6$	$780 \pm 2.6$	$660 \pm 3.8$	$185 \pm 10.8$
6.1	$510 \pm 3.9$	$730 \pm 2.7$	$660 \pm 3.0$	$60 \pm 16.7$
7.2	$465 \pm 4.3$	$585 \pm 4.3$	$400 \pm 5.0$	$5 \pm 40.0$
8.5	$315 \pm 4.8$	$315 \pm 6.3$	$41 \pm 7.3$	$4 \pm 25.0$
9.5	$450 \pm 4.4$	$565 \pm 4.4$	$39 \pm 10.3$	$30 \pm 16.7$

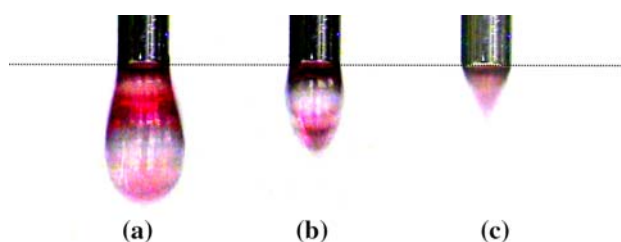


**Fig. 4** The different modes of microbubbling at 1,200  $\mu\text{l/min}$  air flow rate and 300  $\mu\text{l/min}$  lipid flow rate, **a** bubble dripping mode at 2.3 kV, **b** coning mode at 6.9 kV and **c** microbubbling mode at 9 kV. The needle exit is indicated by a dotted line and the needle outer diameter is 1,100  $\mu\text{m}$

voltage and this can be attributed to the loss of the microbubbling mode at higher voltages.

In the case of T-junction microbubbling, monodisperse stable microbubbles  $\sim 100 \mu\text{m}$  in size were obtained (Fig. 5a, b). The polydispersity of obtained bubbles were in range of  $\pm 1\%$ . At the constant liquid flow rate, air pressure was varied until the air stream broke-up in to bubbles and the air stream advanced in to liquid to establish two phase flow. The air column surrounded by slower moving liquid caused resistance to liquid flow upstream. In order to maintain a constant flow rate, the syringe pump keeps on increasing liquid pressure at the junction to deform the air stream and ultimately detach it. The process of break up is typically slow but two-phase flow equilibrium is quick to re-establish. A high-speed camera image (Fig. 5a) of bubble train shows that this typical break-up process repeats at constant time to produce an array of the bubble quanta of similar size. This monodisperse bubble size can be obtained over a narrow air pressure range (see “[Experimental details](#)”) but as air pressure increased beyond this range the monodispersity of bubbles is no longer maintained.

Since this method is taking place in bounded laminar flow, it is unable to rearrange lipid particles at the air–liquid interface spontaneously. Probably layers of viscous liquid flowing parallel to each other around the air column stops particle rearrangement. This also suggests the existence of a laminar region where there is little mass transfer between two consequent layers of liquid flowing over each other. This makes it mandatory to sonicate the suspension before starting to microbubble by T-junction. After using sonicated suspension it was found that these bubbles were remarkably stable while retaining same size over a period of 3 days. Further decrease in the size of microbubbles prepared is possible by reducing the size of the capillaries.

Figure 6 shows the frequency spectra for ultrasound pulses transmitted through: (1) water (2) the phospholipid suspension prior to processing and microbubbles prepared by (3) sonication and (4) T-Junction microbubbling. As may be seen, there is negligible difference between (1) and (2) which indicates that there were very few, if any bubbles



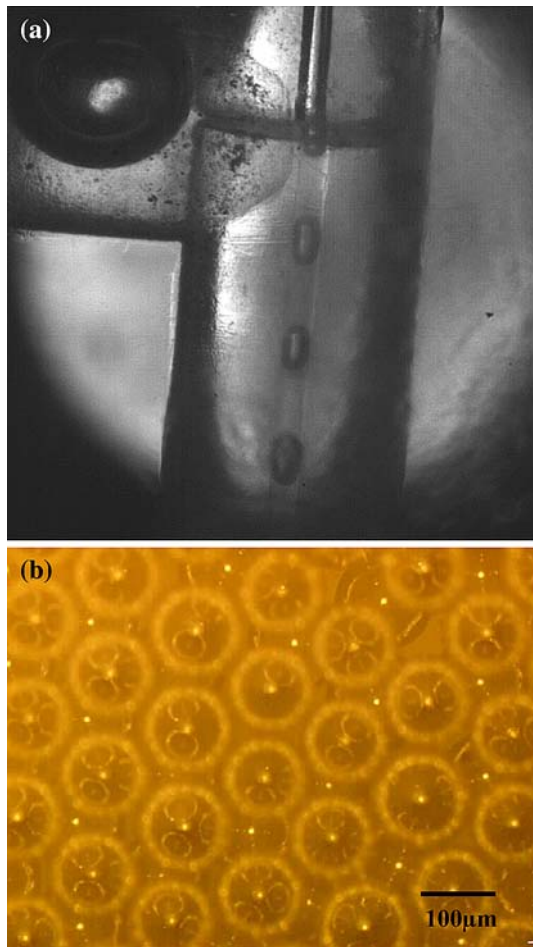


**Fig. 5** **a** High-speed camera image of the T-junction microbubbling in progress and **b** optical micrograph of the bubbles prepared. In **a** the bubbles are in a capillary of 150 µm diameter

present in the phospholipid suspension. The large reduction in signal amplitude for (3) and (4), on the other hand, confirms that microbubbles were successfully prepared by these methods.<sup>2</sup> The difference in amplitude between (3) and (4) may be explained by the fact that the concentration of microbubbles prepared by T-Junction microbubbling was lower than that for sonication and the bubbles were larger and more uniform in size. Consequently, their resonance frequency and amplitude of response would have been much lower and thus the ultrasound would have been less attenuated in propagating through the suspension. The difference in the shape of the spectra for (3) and (4) may also be related to the difference in the size distribution,

<sup>2</sup> It was not possible to make measurements in the microbubble suspensions prepared by co-axial electrohydrodynamic atomization, which were found to be less stable than those prepared by sonication or T-junction microbubbling and thus could not be transferred to the ultrasound characterization apparatus in time. The cause of this instability, which contrasts sharply with that associated with the other methods, is under investigation.

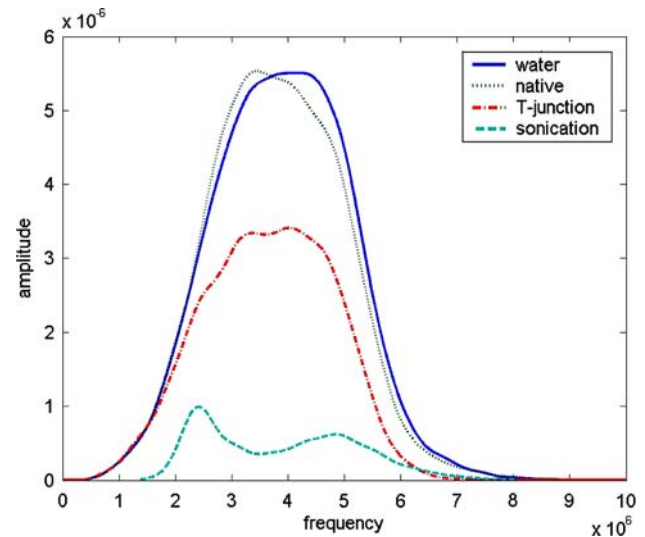


**Fig. 6** Frequency spectra for propagation of a broadband ultrasound pulse (centre frequency 5 MHz, 50 kPa peak negative pressure) through: Water, the phospholipid suspension prior to processing and microbubbles prepared by sonication and T-Junction microbubbling

confirming the importance of controlling this variable for applications of microbubbles in medical ultrasound.

### Concluding remarks

In this work two novel methods for the preparation of uniform size phospholipid coated microbubbles have been demonstrated, both are far superior to the widely used sonication method. The first, co-axial electrohydrodynamic atomization generates <10 µm diameter microbubbles in a well-defined parametric space of the electric field and flow rate of air and suspension. The other, involves using a specially constructed T-junction and gives perfectly mono-disperse microbubbles.

**Acknowledgments** EPSRC (UK) support for this work (grant EP/E01434) is gratefully acknowledged.

### References

- Dayton PA, Ferrara KW (2002) Targetted imaging using ultrasound. *J Mag Resonance Imaging* 16:372–377
- Farook U, Zhang HB, Edirisinghe MJ, Stride E, Saffari N (2007a) Preparation of microbubble suspensions by co-axial electrohydrodynamic atomization. *Med Eng Phys* 29:749–754
- Farook U, Stride E, Edirisinghe M, Moaleji R (2007b) Microbubbling by co-axial electrohydrodynamic atomization. *Med Biol Eng Comp* (in press)
- Hallowell CP, Hirt DE (1994) Unusual characteristics of the maximum bubble pressure method using a Teflon capillary. *J Coll Interf Sci* 168:281–288
- Hettiarachchi K, Talu E, Longo ML, Dayton PA, Lee AP (2007) On-chip generation of microbubbles as a practical technology

- for manufacturing contrast agents for ultrasonic imaging. *Lab Chip* 7:463–468
- Jayasinghe SN, Edirisinghe MJ (2002) Effect of viscosity on the size of relics produced by electrostatic atomization. *J Aerosol Sci* 33:1379–1388
- Klibanov AL (1999) Targeted delivery of gas-filled microspheres, contrast agent for ultrasound imaging. *Adv Drug Delivery Rev* 37:139–157
- Stride E, Saffari N (2003) Microbubble ultrasound contrast agent: a review. *Proc Inst Mech Eng Part H* 217(H6):429–447
- Talu E, Lozano MM, Powell RL, Dayton PA, Longo ML (2006) Long-term stability by lipid coating monodisperse microbubbles formed by a flow-focusing device. *Langmuir* 22:9487–9490
- Unger EC, Hersh E, Vannan M, Matsunaga TO, McCreery T (2001) Local drug and gene delivery through microbubbles. *Progress Cardiovascular Diseases* 44:45–54
- Unger EC, Porter T, Culp W, Labell R, Matsunaga T, Zutshi R (2004) Therapeutic applications of lipid-coated microbubbles. *Adv Drug Delivery Rev* 56:1291–1314